Biotechnology and Bioprocess Engineering 23: 286-292 (2018)
DOI 10.1007/s12257-018-0070-6

pISSN 1226-8372
eISSN 1976-3816

RESEARCH PAPER

Synergistic Transdermal Delivery of Biomacromolecules Using Sonophoresis after Microneedle Treatment

Yeong Chae Ryu, Dong In Kim, Seung Hoon Kim, Hui-Min David Wang, and Byeong Hee Hwang

Received: 1 March 2018 / Revised: 30 April 2018 / Accepted: 1 May 2018

Abstract Transdermal drug delivery systems have been studied as an attractive alternative to conventional delivery routes. However, the outermost layer of the skin, the stratum corneum, acts as a primary barrier to drug delivery. A synergistic combination of microneedles (MNs) and low-frequency ultrasound (U) was used to enhance the penetration of siRNA and ovalbumin. The specific gene knockdown caused by siRNAs through the RNA interference pathway is more stable when delivered via the transdermal route. Ovalbumin, a representative adjuvant, causes a more efficient immune response in the skin because of the numerous immune cells in the skin. The synergistic transdermal delivery resulted in approximately 7 times and 15 times greater penetration of siRNA and ovalbumin respectively than in their respective negative controls, and histological analysis showed minimal invasion. Thus, as the synergistic transdermal delivery enhanced the penetration of biomacromolecules into the skin, this technique is expected to yield a promising technology for a transdermal drug delivery system.

Keywords: transdermal delivery, siRNA, ovalbumin, microneedle, ultrasound

Yeong Chae Ryu, Dong In Kim, Seung Hoon Kim, Byeong Hee Hwang*
Division of Bioengineering, Incheon National University, Incheon 22012, Korea
Tel: +82-32-835-8834; Fax: +82-32-835-2699
E-mail: bhwang@inu.ac.kr

Hui-Min David Wang
Graduate Institute of Biomedical Engineering, National Chung Hsing University, Taichung 402, Taiwan

1. Introduction

The skin is one of the largest organs in the body and may offer a route to replace existing drug delivery pathways [1]. Transdermal drug delivery systems offer major advantages compared to other routes, including increased patient convenience with less pain, avoidance of degradation by the GI tract or enzymes, minimization of systemic toxicity, and easy control of drug absorption [1,2]. In the case of siRNA for local administration, delivered siRNA can be more stable due to direct delivery to target site, and avoidance of intensive enzymatic degradation and high renal and hepatic clearance [3]. Meanwhile, the skin contains many antigen-presenting cells, epidermal Langerhans cells, and dermal dendritic cells. These cells readily take up foreign antigens, migrate to the draining lymph node to present antigens to resting T lymphocytes, and initiate immune responses [4]. Thus, compared to conventional intravascular or intramuscular injection, the transdermal delivery of therapeutic genes or vaccines may be an attractive pathway.

In contrast, the skin functions as a barrier to block drug delivery. The stratum corneum, the outermost layer of the skin, has a structure in which corneocytes are densely packed in a lipid matrix, constituting the 'bricks and mortar'; this is the first major barrier. The cells in the granular layer under the stratum corneum are in tight cell junction formation, which prevents the drug from permeating through the structure [5]. In particular, it is difficult for pharmaceutical biomacromolecules, including nucleic acids or proteins, to penetrate through the skin as it blocks the entry of hydrophilic molecules over approximately 500 Da [6]. The biomacromolecules used for delivery in this study were siRNA and ovalbumin. First, siRNA exerts a major in gene regulation, which is known as RNA

interference (RNAi). It acts to specifically induce the degradation of mRNA, thereby preventing protein translation [7,8]. Second, ovalbumin, a representative protein antigen, has been extensively studied as a model vaccine antigen to induce an immune response [9]. As their size is beyond the range of skin permeability, delivery of proteins is difficult in native form. Therefore, skin penetration techniques are necessary to improve permeation.

The techniques for the improvement of transdermal delivery can be classified into two categories: passive and active methods [10]. Passive methods include the optimization of the drug formulation or delivery vehicle to increase skin permeability. However, these methods offer limited improvement of the skin permeability of biomacromolecules [10]. In contrast, the active methods, which involve a variety of physical or mechanical approaches, demonstrated superior skin permeability, even for biomacromolecules [11]. A simple and direct physical method is the microneedle, which is a needle with a length of approximately 100–700 μm. This form micro-channels in the epidermis, which allows biomacromolecules, including siRNAs and proteins, to penetrate through it [12]. In addition, because the stratum corneum contains no nerves, the skin anatomy provides an opportunity for the microneedles to penetrate through the stratum corneum without pain. Furthermore, microneedles present a much lower possibility of blood-related infection than the hypodermic needle, as no blood vessels exist in the epidermis. However, it offers insufficient drug delivery efficiency within limited application area, and causes little irritation according to biomaterials [13]. Mechanical methods are penetration techniques driven by forces such as electrostatic interactions or ultrasound. Among these methods, sonophoresis improves drug delivery through the formation of micro-channels and cavitation effects by the use of a specific frequency of ultrasound. The skin eventually recovers through natural barrier-recovery mechanisms [14]. Sonophoresis is especially effective at low frequencies (<100 kHz). However, only a limited number of biomacromolecules is delivered, and significant costs are involved [5]. Consequently, although active methods produce a higher penetration of biomacromolecules than passive methods, the development of more efficient skin penetration techniques for use in "real world" settings is necessary.

We have reported that a synergistic combination of microneedle and ultrasound enabled efficient penetration of siRNAs and ovalbumin through the skin. *Ex vivo* experiments checked the permeability of siRNA and ovalbumin through pig skin by sonophoresis after delivery with a microneedle roller. In addition, histological analysis was conducted to confirm whether these combinatorial methods affected the skin tissue.

2. Materials and Methods

2.1. Materials

Cy3-labeled siRNA (5'-GCGACGCUGUCAUCGAUUUTT-3') was synthesized by GenePharma Inc. (Shanghai, China) and Cy3-labeled ovalbumin (OVA) was purchased from Thermo Fisher Scientific (Waltham, MI, USA). Porcine skin pieces of 2.5 cm × 2.5 cm (6.25 cm^2) were purchased from MediKinetics (Pyeongtaek, Korea) and stored in a deep freezer (-80 °C) until use. Prior to the experiment, the porcine skin was thawed in a Petri dish filled with phosphate-buffered saline (PBS) for approximately 1 h. The Franz diffusion cells for skin penetration experiments were purchased from PermeGear, Inc. (Hellertown, PA, USA) and had a receptor volume of 12 mL.

2.2. *Ex vivo* transdermal delivery experiments

Synergistic transdermal delivery was performed by using low-frequency sonophoresis after microneedle treatment (Fig. 1). Porcine skin is commonly used as a model to replace the human skin owing to structural and functional

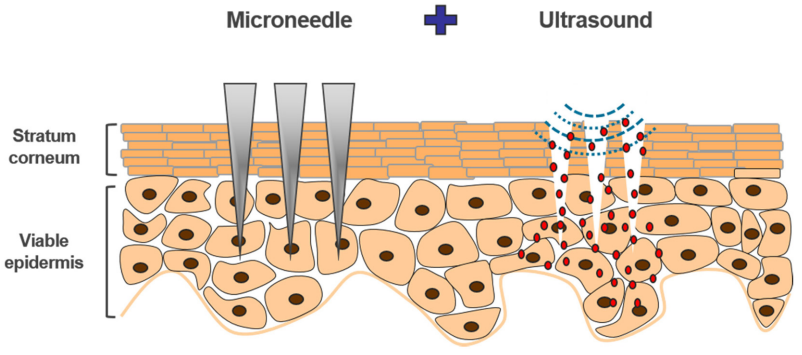

Fig. 1. Illustration of the synergistic principles of microneedles and ultrasound. Microneedles function in a simple and direct manner to provide a passage through which the drug can be delivered via the stratum corneum. Low-frequency ultrasound induces waves and cavitation, which transiently penetrate the stratum corneum and improve the delivery of macromolecules.

suitability. First, the thawed porcine skin was punctured by reciprocating the microneedle roller (Erato International Inc., Seoul, Korea) of 500 μm length while rotating by about 30 degrees for 10 times. Subsequently, it was placed between the donor and receiver parts of the Franz diffusion cell. Sonophoresis was performed in an immersion mode by the addition of 1 mL Cy3-labeled 2.5 nmoL/mL siRNA and 0.5 mL Cy3-labeled 0.2 mg/mL OVA to the donor chamber. Ultrasonic waves at 20 kHz, 20% amplitude, with a 5 s on/off pulse, were applied to the solution in the donor chamber with a 13-mm tip, at a distance of approximately 5 mm for a total of 90 s (on-time) using the ultrasonic liquid processor (VC505, Sonics, Newtown, CT, USA). These sonophoresis conditions were used for the moderate temperature rise up to 37ºC and dominate the cavitation effect for the efficient delivery of biomacromolecules. After sonophoresis treatment, the skin was incubated for 15 min. After all the procedures, the surface of the porcine skin was washed three times with distilled water to remove any solution on the surface and qualitative and quantitative analyses were performed.

2.3. Qualitative and quantitative analysis of skin penetration

The cross-section of the porcine skin was cut thinly with a razor, spread on a slide glass (24 × 40 mm), and covered with a cover glass (18 × 18 mm). The sections were observed by using a fluorescence microscope (TiE, Nikon, Japan) at 200× magnification. For the quantitative analysis, the porcine skin was cut to 0.7 cm × 0.5 cm size and placed in a 2 mL tube with 0.5 mL PBS. The porcine skin pieces were chopped by using fine scissors and ground with a homogenizer (T10 basic Ultra-Turrax®, IKA, Wilmington, NC, USA) for 1 min at intensity 4. After homogenization, centrifugation was performed at 12,032 × g for 10 min. Sixty microliters of the sample supernatant was loaded onto a 384 well-plate (Corning, Inc. Corning, NY, USA) and the fluorescence intensity was repeatedly measured by using a fluorescence-spectrophotometer (Varioskan Flash Multimode Reader, Thermo Fisher Scientific, USA; excitation wavelength, 550 nm; emission wavelength, 570 nm). The samples were analyzed in triplicate. The standard curve was obtained by serial dilution of siRNA and OVA to determine the permeated concentration. All fluorescence experiments were performed in the dark and repeated at least three times.

2.4. Histological analysis of treatment

To investigate the biocompatibility of this synergistic method by using microneedles and low-frequency ultrasound on skin tissue, histological analysis was implemented through hematoxylin and eosin (H&E) staining. The following treatment conditions were analyzed: no treatment, microneedles only, sonophoresis after microneedles; after this, the pieces of porcine skin were trimmed by razor blade. Then, a 10 μm cross-section of the skin was arranged in a cryostat (HM525 NX, Thermo Fisher Scientific, USA). The skin sections were stained with hematoxylin and eosin (Sigma, St. Louis, MO, USA), covered by mounting solution (CC/Mount, Sigma, St. Louis, MO, USA), and then observed by using an optical microscope (CX23, OLYMPUS, Tokyo, Japan).

3. Results and Discussion

3.1. Qualitative analysis of skin penetration

The skin penetration of both siRNA and ovalbumin was enhanced by sonophoresis after microneedle treatment (Fig. 2). The microneedle was used to create multiple micro-channels on the skin without pain. Because the distance between the needles on the microneedle roller is 2 mm and the skin pieces were punched 10 times, the number of total holes was about 200 holes/cm^2. First, the negative control, without any treatment, showed negligible penetration of Cy3-labeled siRNA with fluorescence approximately equal to background noise (Fig. 2A). Cy3-labeled siRNA after microneedle treatment showed increased penetration (fluorescence) in specific skin parts compared with that of the negative control (Fig. 2B). Sonophoresis of Cy3-labeled siRNA after microneedle treatment resulted in the highest epidermal delivery, with a high fluorescence signal over a broad area (Fig. 2C). Next, the negative control, without any treatment, showed slight fluorescence of Cy3-labeled ovalbumin on the skin surface (Fig. 2D). The images of the microneedle treatment show a hole similar to an infundibulum, and ovalbumin can penetrate along this hole (Fig. 2E). The images of the microneedle and ultrasound combination treatment shows the best result, in which ovalbumin penetrated more widely and deeply (Fig. 2F).

3.2. Quantitative analysis of skin penetration

Quantitative analysis was conducted to determine the transmitted amounts of siRNA and OVA. The fluorescence values were measured in the supernatant of homogenized skin with the same area nine times. The fluorescence values were converted into concentration through comparison with a standard curve and plotted in the order of control, microneedle (MN), microneedle and ultrasound (MN & U) method with siRNA (Fig. 3) and OVA (Fig. 4). For the delivery of the siRNA, when the control and MN treatments were compared, the MN treatment (0.074 μM/cm^2) was very slightly higher than the control (0.072 μM/cm^2), but

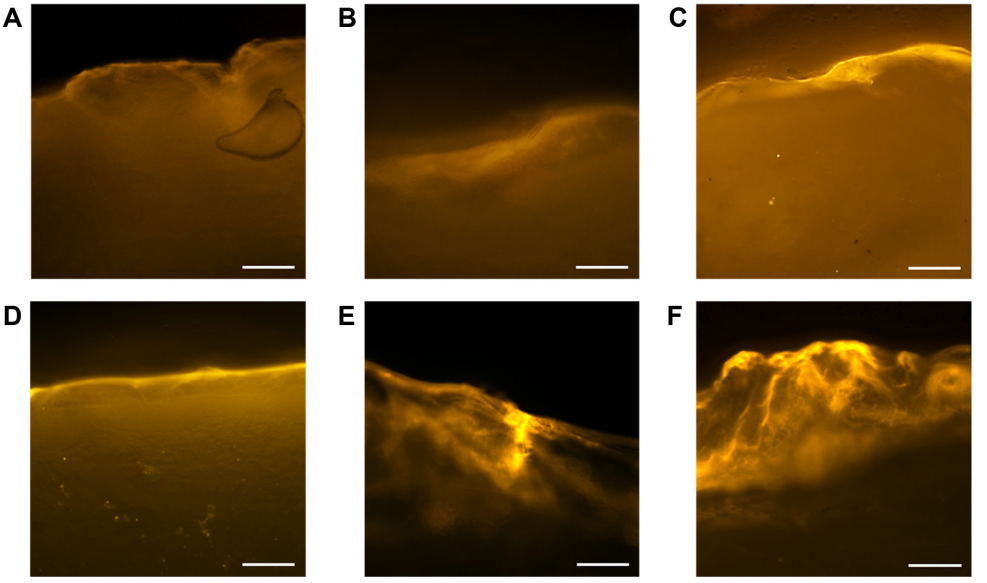

Fig. 2. Skin penetration images of Cy3-labeled siRNA obtained by using fluorescence microscope (TiE, Nikon, Japan). (A) Untreated control, (B) treatment with microneedles only, and (C) treatment with microneedles and ultrasound (Scale bar = 100 μm). Skin penetration images of Cy3-labeled OVA obtained by using a fluorescence microscope. (D) Untreated control, (E) treatment with microneedles only, and (F) treatment with microneedles and ultrasound (Scale bar = 100 μm). The images were obtained with the application of green filter at 200× magnification using excitation wavelength of 550 nm for Cy3.

the difference was not significant, as shown by the t-test. Therefore, the combination method was compared with the MN. The use of sonophoresis after MT treatment showed 6.9-fold higher transmittance (0.51 μM/cm^2) than the MN, which was statistically significant as shown by the t-test.

It is very hard to transfer the test RNA through the skin because it is a hydrophilic macromolecule with a strong negative charge and a molecular weight of approximately 13 kDa. A 2.4- to 10.2-fold increase in transmitted siRNA was reported by using 1.2–1.7 J/cm^2 laser-induced microporation compared with the untreated group [15]. In comparison, in our study, we recorded a 7.1-fold increase in transmitted siRNA compared with the untreated group. Our results reported approximately 0.51 μM/cm^2 of delivered

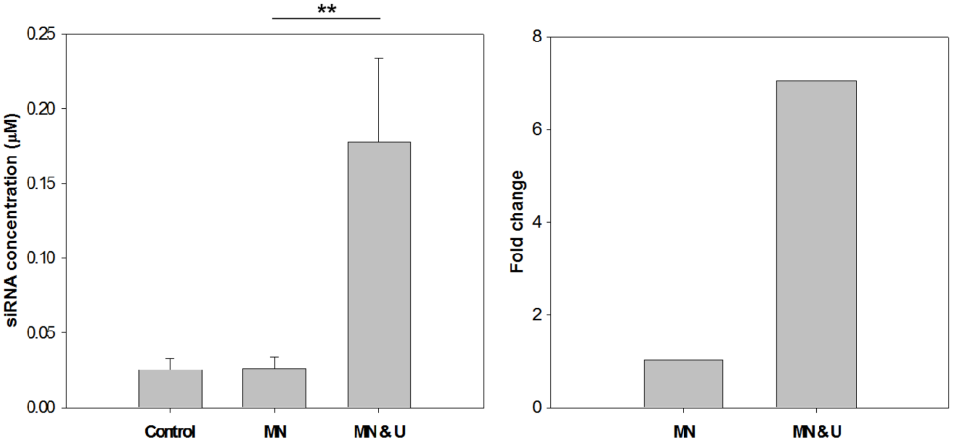

Fig. 3. The concentration of Cy3-labeled siRNA penetrated through porcine skin. Control, No treatment; MN, Microneedle only; MN & U, Microneedle and ultrasound. The fluorescence values were measured by using a fluorescence-spectrophotometer (Varioskan Flash Multimode Reader, Thermo Scientific, USA) after homogenization of the permeated areas of the porcine skin. The graph of the fold changes compares the relative permeability compared with the control (right). MN & U resulted in a 6.9-fold higher concentration of skin penetrated with siRNA than MN. All experiments were repeated nine times to obtain an average value and analyzed statistically. Statistical significance was determined by the t-test ($^{**}p < 0.001$).

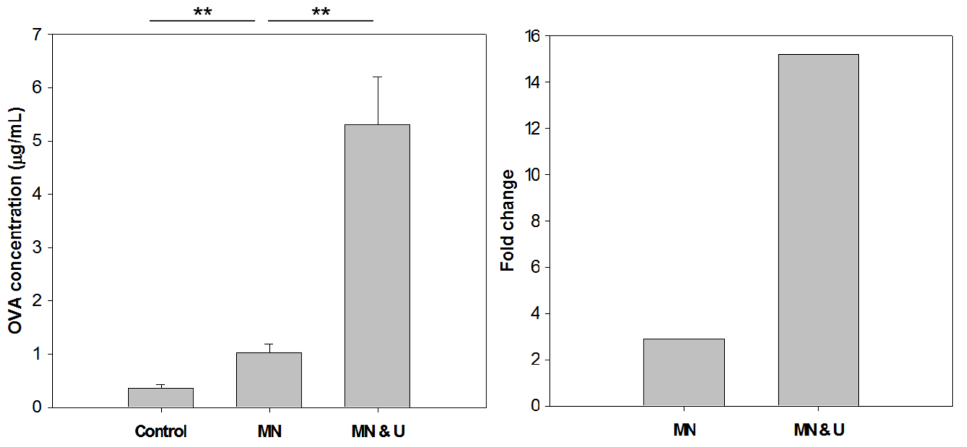

Fig. 4. The concentration of Cy3-labeled OVA penetrated through porcine skin. Control, No treatment; MN, Microneedle only; MN & U, Microneedle & ultrasound. The fluorescence values were measured by using a fluorescence-spectrophotometer (Varioskan Flash Multimode Reader, Thermo Scientific, USA) after homogenization of the permeated areas of the porcine skin. The graph of the fold changes shows a comparison of the relative permeability with the control (right). MN & U resulted in a 5.2-fold higher concentration of skin penetrated by OVA than MN. All experiments were repeated nine times to obtain the average value and analyzed statistically. Statistical significance was determined by the t-test ($^{**}p < 0.001$).

siRNA concentration to the applied siRNA concentration of 1.32 μM/cm^2. Although the two results cannot be directly compared owing to methodological differences, this result was confirmed to show comparably high efficiency of transdermal delivery of siRNA. The mechanism could be explained by the synergistic effects of sonophoresis after MN treatment. MN treatment physically causes micro-scale holes through the epidermal layer of the skin. Sonophoresis generates microscopic shockwaves caused by the collapse of cavitation bubbles. The shockwaves can transfer the macromolecules into the skin through micro-scale holes, hair follicles, and other areas. A similar phenomenon was observed in previous studies, which showed that low-frequency ultrasound caused the penetration of a greater number of microparticles along the hair follicles [16].

For the delivery of the protein, MN treatment (7.4 μg/cm^2) was 2.9-fold higher than the negative control (3.1 μg/cm^2). The MN and ultrasound (20 kHz, 90 s, 4 °C) combination (35.1 μg/cm^2) was 15.2-fold higher than the negative control and 5.2-fold higher than the MN treatment. Significant differences were found between the three experimental conditions, as shown by the t-test (Fig. 4). The protein experiment showed a similar synergistic enhancement of penetration. Ovalbumin, a representative protein for the identification of the immune response, is a hydrophilic 45 kDa molecule. In a previous report, 0.15, 2.4, and 14 μg/cm^2 of transmitted OVA was shown to be proportional to the coated amounts of 0.37, 5.3, and 24 μg/cm^2 using MNs only [17]. Another report showed that 1, 6, and 10 μg/cm^2 of delivered OVA was proportional to the coated amounts of 7.4, 42.2, and 238 μg/cm^2 by using a micro-projection array [18]. On this basis, our results reported approximately 35.1 μg/cm^2 of delivered OVA to the applied amounts of 52.9 μg/cm^2. This synergistic approach showed the highest penetration concentration of OVA and its bioavailability was also maximum level. The explanation of the mechanism would be similar to that mentioned above. In contrast, a stronger fluorescence signal of the protein in the outmost layer of the skin was observed in the negative control than the DNA negative control. This observation could be explained by the nonspecific binding of ovalbumin through hydrophobic interactions.

3.3. Histological observations

Histological observation was performed to investigate the biocompatibility of MNs and low-frequency ultrasound with skin tissue. The H&E-stained skin sections did not show any significant differences between the control, MN, and sonophoresis after MN treatments (Fig. 5). In the images, the upper boundary is the stratum corneum, which is followed by the epidermis and dermis. All pictures showed a clear stratum corneum, without any observable defects. The images of no treatment and MN-only treatment were similar in appearance (Fig. 5A and 5B). In the MN treatment image, the thick bands could be folded cells during cryosection (Fig. 5B). In sonophoresis after MN treatments, the epidermal layer showed micro-apertures and the dermal layer appeared similar to the other conditions (Fig. 5C). The observed circular or oval holes may be hair follicles.

Histological analysis was performed to confirm the biological safety of this method. In the histological images, the dermal layers after each treatment were not observed to

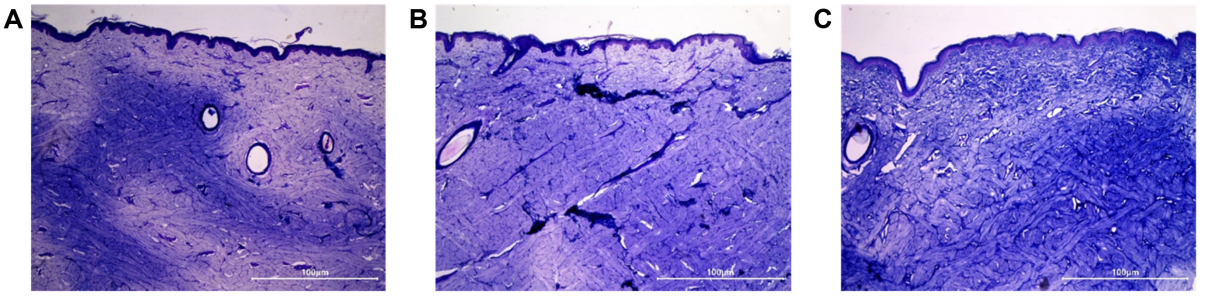

Fig. 5. Histological analysis of treated porcine skins. The skin sections were sliced 10-μm thick by cryostat and stained by hematoxylin and eosin (H&E). Images are (A) untreated control; (B) microneedle only treatment; and (C) Sonophoresis after microneedle treatment. (Scale bar = 100 μm) from left.

be significantly different. The epidermal layer after treatment with the synergistic combination displayed micro-apertures, which could be caused by sonophoresis, as the micro-apertures could be generated by the cavitation effect of low-frequency ultrasound. This might provide an explanation of the superior skin permeability obtained from these synergistic combination. This means that MNs and sonophoresis affected the skin in a minimally invasive manner, but not in an intensively invasive manner. These results were consistent with the results of a previous paper that used low frequency ultrasound with similar conditions (40 kHz, 28% amplitude, and 50% duty cycle) [16]. Minimal invasion of the skin generally recovers within several days [19,20]. Therefore, histological studies have proven that this method is minimally invasive to the skin.

The safety of combinatorial low-frequency sonophoresis and microneedle has not been reported yet. Therefore, we could discuss the safety of each method by references, respectively. For the human skin, microneedle arrays are painless and cause only minimal irritation [21]. The safety of low-frequency sonophoresis has been evaluated in several studies. Singer et al. performed a toxicological analysis of low-frequency sonophoresis. They found a dose-dependent effect of ultrasound on skin and concluded that low-frequency ultrasound at low intensities appears safe for enhancing the topical delivery of medications producing only minimal urticarial reactions [22]. Boucaud et al. also reported no detectable microstructure changes in human skin at an ultrasound of 2.5 W/m2 intensity. Slight and transient erythema and dermal necrosis were observed in hairless rat skin exposed to the same intensity at 24 h [23]. Therefore, ultrasound parameters should be carefully selected in sonophoresis studies.

4. Conclusion

In this study, the synergistic combination of sonophoresis and MN treatment maximized the transdermal delivery efficiency of hydrophilic macromolecules such as siRNA and OVA. The functional mechanism has been proposed by previous studies. The minimal invasiveness of this method was confirmed by histological analysis. The effective topical delivery of biological macromolecules has potential applications in gene therapy or skin immune therapy of various local or systemic diseases. It is also expected that this technology will be a useful tool for drug delivery or biomarker sampling through the skin [24].

Acknowledgments

This research was supported by Basic Science Research Program through the National Research Foundation of Korea (NRF) funded by the Ministry of Science, ICT & Future Planning (NRF-2016R1C1B1014836).

References

1. Prausnitz, M. R., S. Mitragotri, and R. Langer (2004) Current status and future potential of transdermal drug delivery. *Nat. Rev. Drug Discov.* 3: 115-124.
2. Paudel, K. S., M. Milewski, C. L. Swadley, N. K. Brogden, P. Ghosh, and A. L. Stinchcomb (2010) Challenges and opportunities in dermal/transdermal delivery. *Ther. Deliv.* 1: 109-131.
3. Christie, R. J., Y. Matsumoto, K. Miyata, T. Nomoto, S. Fukushima, K. Osada, J. Halnaut, F. Pittella, H. J. Kim, N. Nishiyama, and K. Kataoka (2012) Targeted polymeric micelles for siRNA treatment of experimental cancer by intravenous injection. *ACS Nano.* 6: 5174-5189.
4. Seneschal, J., R. A. Clark, A. Gehad, C. M. Baecher-Allan, and T. S. Kupper (2012) Human epidermal Langerhans cells maintain immune homeostasis in skin by activating skin resident regulatory T cells. *Immunity* 36: 873-884.
5. Zakrewsky, M., S. Kumar, and S. Mitragotri (2015) Nucleic acid delivery into skin for the treatment of skin disease: Proofs-of-concept, potential impact, and remaining challenges. *J. Control.*

Release. 219: 445-456.
6. Hsu, T. and S. Mitragotri (2011) Delivery of siRNA and other macromolecules into skin and cells using a peptide enhancer. *Proc. Natl. Acad. Sci USA*. 108: 15816-15821.
7. Valencia-Sanchez, M. A., J. Liu, G. J. Hannon, and R. Parker (2006) Control of translation and mRNA degradation by miRNAs and siRNAs. *Genes Dev*. 20: 515-524.
8. Castanotto, D. and J. J. Rossi (2009) The promises and pitfalls of RNA-interference-based therapeutics. *Nature* 457: 426-433.
9. Bungener, L., A. Huckriede, J. Wilschut, and T. Daemen (2002) Delivery of protein antigens to the immune system by fusion-active virosomes: a comparison with liposomes and ISCOMs. *Biosci. Rep*. 22: 323-338.
10. Brown, M. B., G. P. Martin, S. A. Jones, and F. K. Akomeah (2006) Dermal and transdermal drug delivery systems: current and future prospects. *Drug Deliv*. 13: 175-187.
11. Mitragotri, S., P. A. Burke, and R. Langer (2014) Overcoming the challenges in administering biopharmaceuticals: formulation and delivery strategies. *Nat. Rev. Drug Discov*. 13: 655-672.
12. Larraneta, E., M. T. McCrudden, A. J. Courtenay, and R. F. Donnelly (2016) Microneedles: A new frontier in nanomedicine delivery. *Pharm. Res*. 33: 1055-1073.
13. Prausnitz, M. R. (2004) Microneedles for transdermal drug delivery. *Adv. Drug Deliv. Rev*. 56: 581-587.
14. Mitragotri, S. (2005) Healing sound: the use of ultrasound in drug delivery and other therapeutic applications. *Nat. Rev. Drug Discov*. 4: 255-260.
15. Lee, W. R., S. C. Shen, R. Z. Zhuo, K. C. Wang, and J. Y. Fang (2009) Enhancement of topical small interfering RNA delivery and expression by low-fluence erbium:YAG laser pretreatment of skin. *Hum. Gene Ther*. 20: 580-588.
16. Paithankar, D., B. H. Hwang, G. Munavalli, A. Kauvar, J. Lloyd, R. Blomgren, L. Faupel, T. Meyer, and S. Mitragotri (2015) Ultrasonic delivery of silica-gold nanoshells for photothermolysis of sebaceous glands in humans: Nanotechnology from the bench to clinic. *J. Control. Release* 206: 30-36.
17. Matriano, J. A., M. Cormier, J. Johnson, W. A. Young, M. Buttery, K. Nyam, and P. E. Daddona (2002) Macroflux microprojection array patch technology: a new and efficient approach for intracutaneous immunization. *Pharm. Res*. 19: 63-70.
18. Widera, G., J. Johnson, L. Kim, L. Libiran, K. Nyam, P. E. Daddona, and M. Cormier (2006) Effect of delivery parameters on immunization to ovalbumin following intracutaneous administration by a coated microneedle array patch system. *Vaccine* 24: 1653-1664.
19. Mitragotri, S., D. Blankschtein, and R. Langer (1996) Transdermal drug delivery using low-frequency sonophoresis. *Pharm. Res*. 13: 411-420.
20. Polat, B. E., D. Blankschtein, and R. Langer (2010) Low-frequency sonophoresis: application to the transdermal delivery of macromolecules and hydrophilic drugs. *Expert Opin. Drug Deliv*. 7: 1415-1432.
21. Bal, S. M., J. Caussin, S. Pavel, and J. A. Bouwstra (2008) In vivo assessment of safety of microneedle arrays in human skin. *Eur. J. Pharm. Sci*. 35: 193-202.
22. Singer, A. J., C. S. Homan, A. L. Church, and S. A. McClain (1998) Low-frequency sonophoresis: pathologic and thermal effects in dogs. *Acad. Emerg. Med*. 5: 35-40.
23. Boucaud, A., J. Montharu, L. Machet, B. Arbeille, M. C. Machet, F. Patat, and L. Vaillant (2001) Clinical, histologic, and electron microscopy study of skin exposed to low-frequency ultrasound. *Anat. Rec*. 264: 114-119.
24. Paliwal, S., B. H. Hwang, K. Y. Tsai, and S. Mitragotri (2013) Diagnostic opportunities based on skin biomarkers. *Eur. J. Pharm. Sci*. 50: 546-556.